Available online at www.sciencedirect.com
SCIENCE DIRECT
Journal of Membrane Science 278 (2006) 457–463
journal of MEMBRANE SCIENCE
www.elsevier.com/locate/memsci

Development of charged ion exchange resin-polymer ultrafiltration membranes to reduce organic fouling

N.A. Ochoa *, M. Masuelli, J. Marchese

Laboratorio de Ciencias de Superficies y Medios Porosos, UNSL-CONICET-FONCYT, Chachabuco 917, 5700 San Luis, Argentina

Received 2 September 2005; received in revised form 10 November 2005; accepted 18 November 2005
Available online 20 December 2005

Abstract

This work deals with the performance of polymeric membranes charged with an ion exchange resin on the ultrafiltration (UF) of an oily suspension. The membranes were prepared by the phase inversion process from polysulfone (PSf) solutions and different percentages of resin. The structural and functional study of membranes was carried out by SEM, dextran rejection, streaming potential (SP), oil content and chemical oxygen demand (COD). The structural study showed that there is an important change of the porous membrane substructures leading to a higher densification when the resin content increases. The results showed that the membrane propensity fouling decreased with increasing resin concentration (1–20 wt.% resin). The best performance—less membrane fouling and better permeate quality—was obtained with the membrane prepared with 20 wt.% resin.

Keywords: Ultrafiltration; Fouling; Charged membrane; Cation exchange resin

1. Introduction

The reuse of water is crucial for lowering costs of industrial process and avoiding the water waste in zones of water shortage. The application of membrane technology in the treatment of water includes pathogen and natural organic matter (NOM) removal [1–4], and treatment of oily emulsions [5–8]. Although the use of membrane processes is well known for a long time, specially the use of ultrafiltration for the treatment of effluents [9], with respect to the economy as well as to the speed of the process, the fundamental factor is the membrane itself since it determines the fouling—the limiting phenomenon of this application. This phenomenon can be reduced three-fold: (a) by operational conditions varying the pressure or feed flow [10,11], (b) by pretreatment which includes the addition of flocculants [10,12], and (c) by the modification of the surface chemical characteristics of the membrane, minimizing the membrane–solution interaction [13,14]. In general, membrane functionality may be carried out by several methods of grafting: ionizing radiation, plasma, oxidants and redox systems or UV radiation [14–19]. The grafting consists in adding a hydrophilic chain or electrostatically charged group.

Due to the concurrence of two phenomena—exclusion by size and by electrostatics—charged membranes have been developed mainly for the separation of charged solutes such as proteins [20,21]. Van Reis et al. [22] used membranes Biomax^{TM} for the separation of proteins with similar size. Their studies focused on exploring the effect of membrane charge, in combination with buffer pH on protein separation using high performance tangential flow filtration. As a conclusion, the authors provided an important insight into the nature of electrostatic interactions controlling transmission of charge proteins through charged membranes. The membrane charge should be of the same sign as the charge on the product protein at the selected pH value to enhance the electrostatic exclusion of the product from the membrane pores. Möckel et al. [23] prepared membranes of UF with the increase of hydrophilicity made from chemically modified polysulfone (PSF). Hydrophilised polysulfones show less static adsorption and lower UF flow reduction than hydrophobic and modified membranes. In all experiments, it was found that the higher the degree of carboxylation or sulfonation, the greater is this effect. Hosch and Staude [24] modified polyamide membranes with both positively and negatively charged substituents. The charged polyamide membranes were less prone to

* Corresponding author. Tel.: +54 2652 424689; fax: +54 2652 430224.
E-mail address: aochoa@unsl.edu.ar (N.A. Ochoa).

0376-7388/$ – see front matter © 2005 Elsevier B.V. All rights reserved.
doi:10.1016/j.memsci.2005.11.032

adsorptive fouling by human serum albumin than their unmodified counterparts.

The development of ultrafiltration charged membranes for water treatment has been less studied. Bowen et al. [25] reported membranes made from blends of polysulfone and sulfonated poly(ether, ether ketone) with high charge and porosity. These membranes showed high retention of humic acid and low fouling properties. In addition, humic acid deposits formed on the charged membranes above the critical fluxes had a loose structure and were consequently, efficiently removed by rinsing. Carroll et al. [26] developed charged and non-charged hydrophilic polymers, which were grafted as a flexible layer onto a polypropylene hollow fiber. Non-cationic and cationic hydrophilic grafts have rates of flux decline by NOM fouling up to 50%, lower than ungrafted polypropylene. Anionic hydrophilic grafts have initial flux increase up to 140% at high graft yields due to multi-valent ions in natural water, although the pure-water flux is substantially lower than for the ungrafted membrane.

Taniguchi et al. [14] evaluated six different hydrophilic monomers for their ability to reduce fouling by NOM: two neutral monomers, two weakly acidic (carboxylic) monomers, and two strongly acidic (sulfonic) monomers. Grafting increased membrane surface wettability and shifted the membrane pore size distribution to smaller sizes. Reversible fouling resulting from cake formation was only weakly dependent on membrane surface chemistry; in contrast, irreversible fouling exhibited a marked dependence on surface chemistry. They concluded that wettability (or hydrophilicity) is not an appropriate parameter for estimating reduced fouling potential for NOM feed. They hypothesized that this is a consequence of the structural and chemical heterogeneity of NOM.

Although Akthakul et al. [27] did not use charged but functionalized membranes, they described polymer thin film composite membranes coated with amphiphilic graft copolymers consisting of a poly(vinylidene fluoride) PVDF backbone and poly(oxyethylene methacrylate) POEM side chains. These membranes wet instantaneously and reject <99.9% of emulsified oil from 1000 ppm oily water microemulsion feed without fouling.

This kind of modifications is not easy to carry out, and this type of membranes has a high-cost production.

In this work, the preparation of PSf charged membranes by adding resins to a polymeric solution is proposed. The effect of resin concentration on both the membrane structure and functional behavior has been analyzed. To evaluate their fouling behavior and performance, synthesized membranes were used to filtrate an oily emulsion.

2. Experimental

PSf UDEL® P-3500 was provided by Amoco, Polyvinylpyrrolidone (PVP) K30, Dextrans: 8.8, 40, 70, 200, 2000, 4900 KDa, and DOWEX® 50WX8 strongly acidic resin were purchased from Fluka. *N*,*N*-dimethylformamide (DMF), KCl, KOH, HCl were provided by Merck. Commercial emulsive oil (Insignia® oil) was purchased from JyM Lubricantes S.A (Argentina). Viledon 2431 non-woven support was kindly provided by Carl Freudenberg, Germany.

Table 1
Casting solution composition

Membrane	PSf (wt.%)	PVP K30 (wt.%)	Weight ratio CR:PSf	DMF (wt.%)
PSf	20	5	0:100	75
PSfC1			1:99	
PSfC10			10:90	
PSfC20			20:80	

2.1. Preparation of charged membranes

The general preparation procedure is as follows: PSf and PVP are dissolved in DMF, after that the ionic exchange resin is added to the solution. The final mixture was cast onto the non-woven support using a film extensor. The solution is then coagulated with bidistilled water at 25 °C. Afterwards membranes are stored in a water bath until being used. Table 1 shows the different cation resin (CR) composition of each membrane.

2.2. Microscopy

Scanning electron microscopy images were obtained using an EVO40 Carl Zeiss microscope (Cambridge, London). Membrane samples were freeze-fractured and then coated by sputtering a thin gold layer. They were observed under high vacuum.

2.3. Tangential flow streaming potential measurements

The streaming potential (SP) on the membrane was measured by using a membrane holder where two membrane samples were placed by facing their active layers with no permeation allowed through them. Pt electrodes have been used and electric potentials measured by using a high-impedance voltmeter Model Fluke 45 from Fluke Corporation, with an accuracy of 1 μV. The pH of the 0.001 M of the KCl solutions was adjusted by adding small amounts of 1 M HCl or KOH and measured using a pH-meter Orion (model 230A). The membrane under investigation was always fresh and soaked overnight in 0.001 M KCl solution to equilibrate it with the measuring solution.

2.4. Filtration experiments

All experiments of filtration were carried out in a Minitan-S ultrafiltration device from Millipore Corp. The experimental protocol was as follows:

First, the membrane was compacted at 100 KPa pressure of transmembrane during 30 min [28]. Then, different pressures from 100 to 20 KPa were applied measuring the corresponding pure-water fluxes. Once the hydraulic permeabilities were determined, measurements with dextrans were carried out using a dextran molecular weight ranging from 8 to 4900 KDa, according to a method reported elsewhere [8,29]. Dextran concentrations were determined using a HPLC from Gilson coupled to a

refraction index. The distribution of pore radius can be summarized as follows:

$$f_d = \frac{d(J_{w,t}/J_w)}{d(r_p)} \quad (1)$$

where $J_{w,t} = J_v(1-R)$, J_v is the permeate flux, R the retention coefficient, and $J_w = J_v - J_s$ with $J_s = J_v C_p$. The porous radius r_p can be related to the molecular size of dextran molecule by

$$r_p = 0.4253(MW)^{0.45} \quad (2)$$

Once measurements were carried out, the membrane was mechanical cleaned with pure water for 1 h at 67 KPa with a feed flow of 1 L/min. After that, no fouling was observed. Then, fouling test experiments with oil emulsion were performed for 2 h at the same pressure and feed flow. After that, the membrane was cleaned with pure water at high feed rate. Finally, pure-water flow was measured under the same emulsion conditions.

2.5. Emulsion characteristics

Emulsion was obtained adding Insignia® oil to distillated water at 500 rpm. The emulsion with a 0.1% oil/water concentration had 2.5 μm diameter of average oil droplet size with standard desviation of 2.26 measured with a Carl Zeiss Pol II microscope. The droplet size distribution is showed in Fig. 1.

The electrophoretic mobility of emulsion drops were determined using a Beckman P/ACE MDQ instrument (Beckman Instruments, Inc. Fullerton, CA) equipped with a diode array detector and a handling system comprising an IBM personal computer and P/ACE System MDQ software. The fused silica capillaries were obtained from MicroSolv Technology Corp. Electroosmotic flow (EOF) determination was performed by using acetone as an EOF marker. Zeta potential of emulsion was obtained using the well-known equation of Helmholtz–Smoluchowski. Fig. 2 shows zeta potential versus pH, calculated from mobility data.

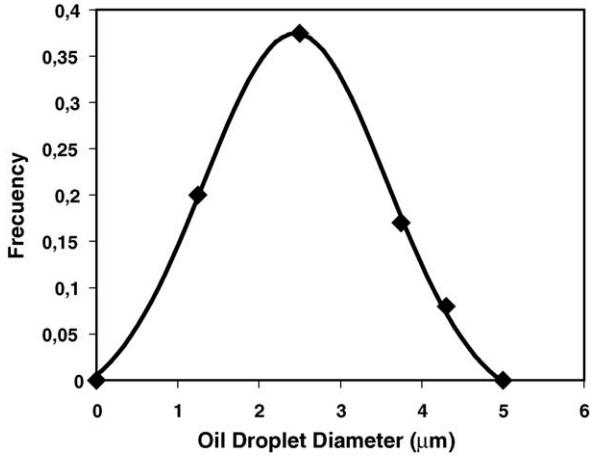

Fig. 1. Emulsion drop size distribution from optical microscopy.

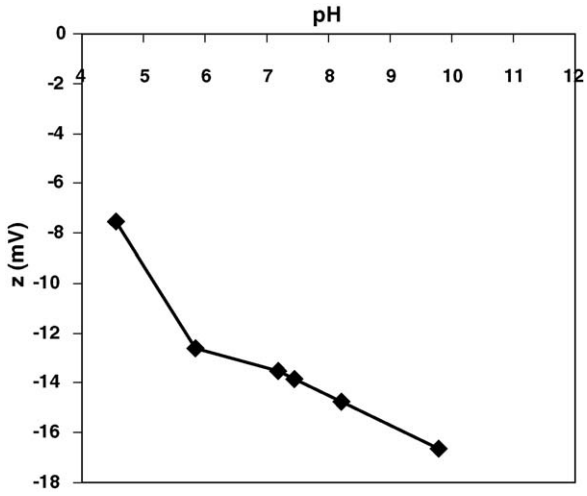

Fig. 2. Zeta potential of emulsion vs. pH.

2.6. Chemical oxygen demand (COD)

Samples were refluxed in strongly acid solution with a predetermined excess of potassium dichromate. Consumed oxygen was measured against standards at 600 nm by U-2001 UV–vis Hitachi spectrophotometer (5220D Standard Method for the Examination of Water and Wastewater).

2.7. Oil content

Oil content was evaluated by UV–vis spectroscopy based on wavelength of 220 nm.

3. Results and discussion

Fig. 3 shows SEM images of membrane cross-sections. There is a noticeable variation in the membrane structure from a finger-like morphology for a non-resin membrane (PSf) to a more densified structure for PSfC20 membrane. This effect is similar to that found by other authors [30] where a decrease of macrovoids in the porous substructure was obtained by adding water to casting solution. This also seems to be our case since exchange resins adsorbed easily water from the air during their storage. The adsorbed water in the resin would produce an increase of the casting solution viscosity causing a decrease of the mass transfer rate during coagulation and consequently, a decrease in the macrovoid formation.

A consequence of this trend is the decrease of hydraulic permeability as the resin content increases with a variation from 4.22 to 0.40×10^{-10} m/s Pa for PSf and for PSfC20, respectively. These results can be seen in Table 2.

However, this porous structure densification does not produce a decrease of the pore size. Fig. 4 shows the distributions of pore radius obtained from dextran rejection measurements. In this figure, a shift to larger pore sizes can be observed when the resin content increases. In the case of the membrane with 20 wt.% resin, a bimodal distribution was found with a maximum at 1.70 nm and another at 8 nm. Mean radios pore are shown

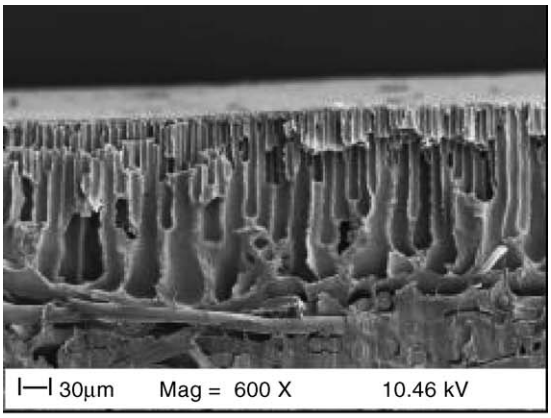

(a)

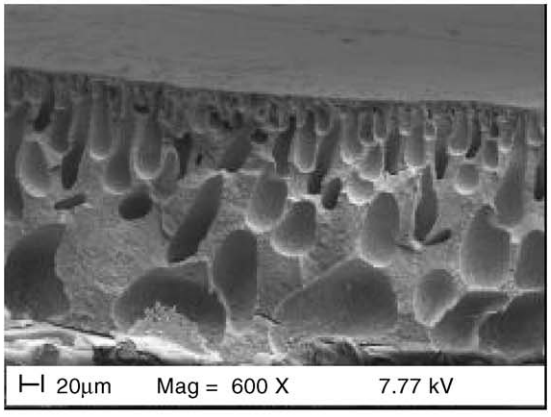

(b)

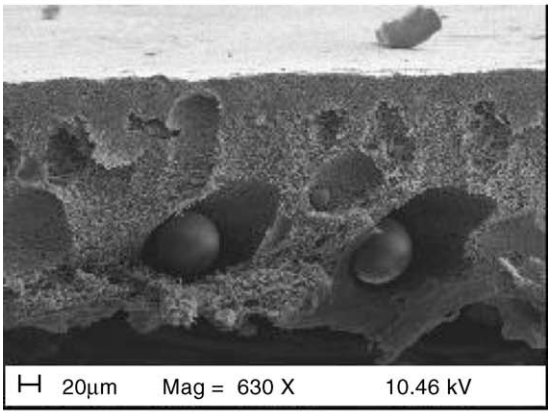

(c)

Fig. 3. SEM cross section structure micrograph of: (a) PSf; (b) PSfC1; (c) PSfC20.

Table 2
Membrane hydraulic permeability and mean pore size

Membrane	r_{mp} (nm)	Lhi $\times 10^{10}$ (m^3/m^2 Pa s)
20PSf	1.81	4.22
20PSfC1	2.54	9.50
20PSfC10	3.17	1.24
20PSfC20	3.41[a]	0.40

[a] Bimodal distribution.

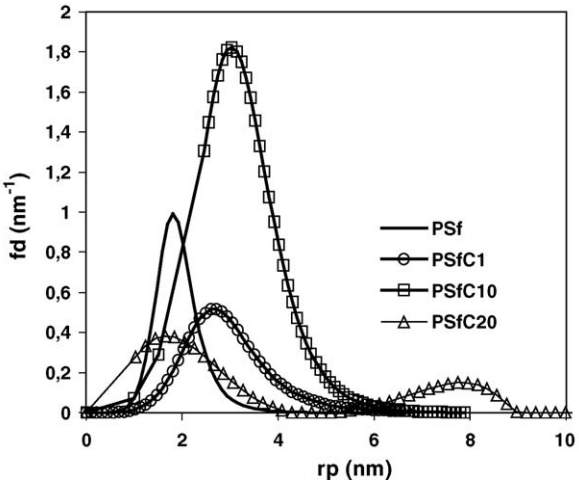

Fig. 4. Pore size distribution of prepared membrane.

in Table 2. Resin particles create zones of discontinuity in the polymeric solution such as void spaces between resin particles and the polymeric matrix during the phase inversion process. A low adhesion between resin-polymer phases produces larger pore size.

The electrokinetic characterization of membranes involves several techniques, such as electroosmosis, electroviscous effect, streaming potential, and potentiometric titration. Due to its versatility, streaming potential is the most used method for electrokinetic characterization of membranes. Zeta potential can also be obtained by using Helmholtz–Smoluchowski technique. However, when charged membranes are measured, surface conduction phenomenon becomes important. Möckel et al. [23] compared both zeta potentials—those calculated taking into account the contribution of surface conduction and those calculated neglecting that contribution. The surface conduction contribution is measured by membrane resistance when there is no liquid flow using an AC bridge. However, this correction is carried out taking into account the zeta potential equation although SP remains unaltered by this situation. For that reason, we report the data of SP. Fig. 5 shows the variation of SP as a function of the pH for prepared membranes. The PSf membrane has its isoelectric point at pH 5, consistent with other author's results [23,31,32]. Charged membranes have a negative SP in all the pH range, and SP becomes smaller as pH increases. This behavior was also obtained by Mockel et al. [23] when using carboxylated PSf, and by Rodemann and Staude [33] when an epoxided PSf membrane reacted with iminodiacetic acid was electrokinetically characterized.

Fig. 5 also shows that as resin content increases in the membrane, SP decreases. Jacobash and Börner [34] found similar results for sulfonated polyethersulfone membranes having a zeta potential decrease when the membrane electrostatic charge increases. They assume that the extraordinary hydrophilicity of the sulfonic acid groups increases the thickness of the swelling layer concerned with the membrane surface. As a result, the shear plane is moved towards the solution bulk and, thus, a lower zeta potential is eventually measured. Szymczyk et al. [35] showed the distribution of the electrostatic potential (Ψ)

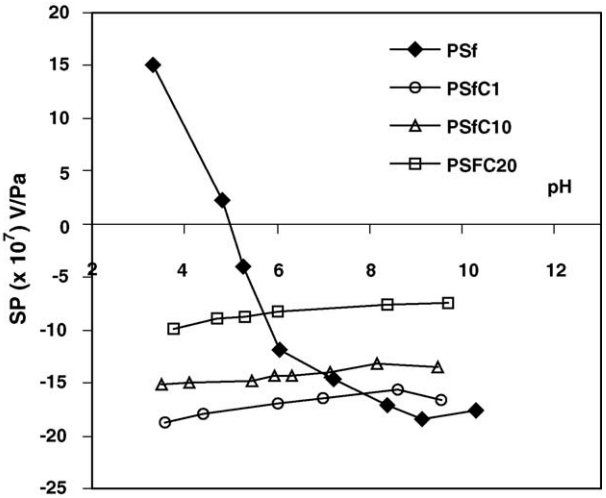

Fig. 5. Streaming potential vs. pH ([KCl] = 0.001 M).

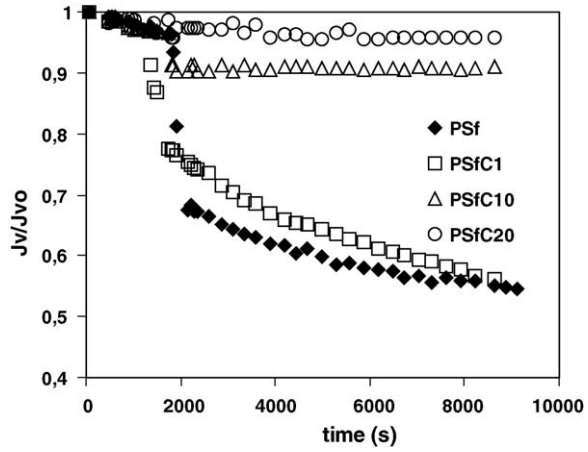

Fig. 6. Normalized flux decline for the different membranes studied.

by pores of different sizes obtained by the non-linear equation of Poisson–Boltzmann and the variation of Ψ with the zeta potential. For small pores, $r_p = 2$ nm, the radius variation of Ψ is small and the assumption of a constant potential is reasonable. In this case, the assumption of a Donan partition at the entrance of the pore can be justified. However, this assumption is true for low zeta potentials while with high zeta potentials, the radius variation of Ψ becomes significant as the zeta potential increases. Obviously, this would produce a deviation of Helmholtz–Smoluchowski equation, which considers that zeta potential is directly proportional to SP, independently of the electrokinetic radius. Helmholtz–Smoluchowski relation assumes that the conductivity in the pore is the same as in the solution, but in small pores and at high zeta potentials, the conductivity in the pore is substantially higher than in the solution. A number that reflects this situation is Dukhin number, defined as:

$$\mathrm{Du} = \frac{G_s}{\lambda_0 r_p} \tag{3}$$

where G_s is the surface conductance, and λ_0 is the conductivity of the electrolyte in solution. Szymczyk et al. [35] showed that for small pores, $r_p/k^{-1} = 0.5$ (where k^{-1} is the Debye's length) and an electrolyte concentration of 0.001 M, Du number increases abruptly with the zeta potential. In this case, conduction takes place mainly along the charged surface as seems to be the case in this work with prepared membranes. As a consequence of this effect, it was found that SP has a maximum with respect to G_s where SP decreases from that maximum in spite of the increase of G_s. This would explain the results obtained with our membranes in which an increase in the resin concentration produces a lower SP value.

3.1. Fouling

Fig. 6 shows the normalized flow decline of the oily effluent with prepared membranes. There is a more marked flow decline in the non-charged membrane, and therefore a higher fouling. As the resin content in the membrane increases, this decline becomes less and less sharp, until the fouling phenomenon disappears in PSfC20 membrane.

Mass permeation flux during filtration can be expressed in terms of a resistance model as

$$J_v = \frac{\Delta P}{\mu R_T} = \frac{\Delta P}{\mu(R_M + R_F)} \tag{4}$$

where J_V is the permeate flux (m^3/m^2 s), ΔP the applied pressure (Pa), R_T the total resistance of permeation (m^{-1}), and μ (Pa s) is the permeate viscosity. R_T involves the intrinsic resistance of membrane, R_M, and the fouling resistance, R_F. The osmotic effect, the effect of polarization by concentration, and the effect of fouling are all included in R_F, which is subdivided into reversible fouling (R_{revF}) and irreversible fouling (R_{irrevF}).

$$R_F = R_{revF} + R_{irrevF} \tag{5}$$

Reversible fouling resistance due to loosely attached foulants is considered to be easily removed by "flushing" the membrane with distillated water, where a strong shear force corresponding to a high cross-flow velocity is applied to clean the fouled membrane surface. Thus, the irreversible fouling due to strong attachment of foulants still remains after flushing.

Table 3 shows the resistances found during filtration. As mentioned above, there is an increase of R_M due to a structural change of the membrane as resin content was increased. Increasing the electrostatic charge of membranes, a decrease of the fouling can be observed. Thus, for non-resin membrane (PSf) and low electrostatic charge membrane (PSfC1), there is a reversible as well as irreversible fouling. In the case of PSfC10 membrane only a reversible fouling is observed, while in the

Table 3
Membrane and fouling resistances

Membrane	$R_M \times 10^{-11}$ (m^{-1})	$R_F \times 10^{-11}$ (m^{-1})	$R_{revF} \times 10^{-11}$ (m^{-1})	$R_{irrerF} \times 10^{-11}$ (m^{-1})
PSf	22.80	16.30	11.10	5.31
PSfC1	14.90	11.30	4.11	7.11
PSfC10	69.80	15.10	15.10	0.00
PSfC20	482.00	0.00	0.00	0.00

Table 4
COD permeate and oil rejection of membranes prepared

Membrane	COD permeate (ppm)	Oil rejection %
PSf	119	89.00
PSfC1	79	93.68
PSfC10	76	93.92
PSfC20	73	94.30

PSfC20 membrane there is no fouling at all. This indicates that in charged membranes, the electrostatic exclusion is a predominant factor in the filtration of this emulsion. In this case, at pH 7, emulsion particles and charged membranes have zeta potentials of the same sign. As a result, the membrane with higher ion exchange resin concentration (PSfC20) do not show a permeate flow decrease, evidencing the absence of fouling phenomenon. This phenomenon of electrostatic exclusion was studied by Mehta and Sydney [36] who showed the advantage of using charged membranes in protein separation. When using a negatively charged membrane for BSA ultrafiltration at pH 7 (BSA negatively charged), a sharp difference in the curve between selectivity and permeability was obtained due to a dramatic change in the separation factor because of the electrostatic exclusion.

In our case, this effect seems to be confirmed observing the permeate quality given by COD values. The COD value for feed emulsion was 1700 ppm. Table 4 shows that starting from a permeate COD value of 119 ppm for the non-charged membrane this value decreases to 73 ppm for the membrane with a 20% of resin. As described above, PSf membrane has the smallest pore size and it increases as the resin content increases as well, i.e., COD decrease in the permeate increasing resin content is the result of electrostatic exclusion. Therefore, it is possible to increase COD retention even with a larger pore size and consequently, to improve the permeate quality. The same behavior was observed when the oil permeate concentration is analyzed (Table 4). In this case, the oil rejection varied from 89 to 94% for PSf and PSfC20 membranes, respectively.

4. Conclusions

Membranes with different contents of ion exchange resins were prepared. The presence of resins produces membranes with higher pore sizes and less permeabilities due to the porous substructure densification. In the case of the membrane with 20% resin content, a bimodal pore distribution was obtained with average pore radius of 2.50 and 8 nm for each peak, respectively.

Streaming potential values decrease as the content of charges increases as a result of high surface conductivity. The ultrafiltration experiments show different types of fouling, i.e., both reversible and irreversible fouling in low-charged membranes (pure PSf and PSfC1); reversible fouling in PSfC10 membrane; and no fouling in high-charged membrane (PSfC20). An increasing electrostatic repulsion due to the increase of resin content resulted in a permeate solution with lower both COD values and oil concentration.

References

[1] B. Fan, X. Huang, Characteristics of a self forming dynamic membrane coupled with a bioreactor for municipal wastewater treatment, Environ. Sci. Technol. 36 (2002) 5245–5251.
[2] G.A. Cho, J. Pellegrino, Membrane filtration of natural organic matter: initial comparison of rejection and flux decline characteristics with ultrafiltration and nanofiltration membranes, Water Res. 33 (11) (1999) 2517–2526.
[3] C.-F. Lin, Y.-J. Huang, O.J. Hao, Ultrafiltration processes for removing humic substances: effect of molecular weight fractions and PAC treatment, Water Res. 33 (1999) 1252–1264.
[4] M. Tiniguchi, J.E. Kilduff, G. Belfort, Modes of natural organic fouling during ultrafiltration, Environ. Sci. Technol. 37 (2003) 1676–1683.
[5] P. Jancknecht, A.D. Lopez, A.M. Mendes, Removal of industrial cutting oil from oil emulsions by polymeric ultra-and microfiltration membranes, Environ. Sci. Technol. 38 (18) (2004) 4878–4883.
[6] M. Gryta, K. Karakulski, A.W. Morawski, Purification of oily wastewater by hybrid UF/MD, Water Res. 35 (15) (2001) 3665–3669.
[7] J. Mueller, Y. Cen, R.H. Davis, Crossflow microfiltration of oily water, J. Memb. Sci. 129 (1997) 221–235.
[8] N.A. Ochoa, M. Masuelli, J. Marchese, Effect of hydrophilicity on fouling of an emulsified oil wastewater with PVDF/PMMA membranes, J. Memb. Sci 226 (2003) 203–211.
[9] J. Mallevialle, P. Odendaal, M.R. Wiesner (Eds.), Membrane Processes in Water Treatment, McGraw-Hill, 1996.
[10] J. Marchese, N. Ochoa, C. Pagliero, C. Almandoz, Pilot scale ultrafiltration of an emulsified oil wastewater, Environ. Sci. Technol. 34 (14) (2000) 2990–2996.
[11] M. Minhalma, M.N. de Pinho, Flocculation/flotation/ultrafiltration integrated processes for the treatment of cork processing wastewaters, Environ. Sci. Technol. 35 (2001) 4916–4921.
[12] H.K. Shon, S. Vinegswaran, H.H. Ngo, R. Ben Aim, Is semi-flocculation effective as pretreatment to ultrafiltration in wastewater treatment? Water Res. 39 (2005) 147–153.
[13] J. Gilron, J. Belfer, Y. Purinson, M. Vaisanen, M. Nystrom, Effect of surface modification on antifouling and performance properties of reverse osmosis membranes, Desalination 139 (2001) 169–176.
[14] M. Taniguchi, J.E. Kilduff, G. Belfort, Low fouling synthetic membranes by assisted graft polymerisation: monomer selection to mitigate fouling by natural organic matter, J. Memb. Sci. 222 (2003) 59–70.
[15] S. Kiyohara, M. Kim, Y. Toida, K. Saito, K. Sugita, T. Sugo, Selection of a precursor monomer for the introduction of affinity ligands onto a porous membrane by radiation-induced graft polymerization, J. Chromatogr. A 758 (1997) 209–215.
[16] S. Belfer, Y. Purinson, O. Kedem, Surface modification of commercial polyamide reverse osmosis membranes by radical grafting: an ATR-FTIR study, Acta Polym. 49 (1998) 574–582.
[17] D.S. Wavhal, E.R. Fisher, Hydrophilic modification of poly(eter sulfone) membranes by low temperature plasma-induced graft polymerisation, J. Memb. Sci. 209 (2002) 255–269.
[18] M. Taniguchi, J. Pieracci, W.A. Samsonoff, G. Belfort, UV-assisted graft polymerization of synthetic membranes: mechanistic studies, Chem Mater. 15 (2003) 3805–3812.
[19] J. Pieracci, J. Crivello, G. Belfort, *N*-vinyl-2-pyrrolidinone onto poly(ether sulfone) ultrafiltration membranes using selective UV wavelengths, Chem. Mater. 14 (2002) 256–265.
[20] H. Chen, G. Belfort, Surface modification of poly(ether sulfone) ultrafiltration membranes by low-temperature plasma-induced graft polymerisation, J. Appl. Polym. Sci. 72 (1999) 1699–1711.
[21] Y. Wang, J.-H. Kim, K.-H. Choo, Y.-S. Lee, C.-H. Lee, Hydrophilic modification of polyprolilene microfiltration membranes by ozone-induced graft polymerisation, J. Memb. Sci 172 (2000) 269–276.
[22] R. van Reis, J.M. Brake, J. Chaurkodian, D.B. Burns, A.L. Zydney, Zydney. High performance tangential flow filtration using charged membranes, J. Memb. Sci. 159 (1999) 133–142.

[23] D. Möckel, E. Staude, M.D. Guiver, Static protein adsorption, ultrafiltration behavior and cleaneability of hydrophilized polysulfone membranes, J. Memb. Sci. 158 (1999) 63–65.
[24] J. Hosch, E. Staude, Preparation and investigation of chemically modified porous polyamide ultrafiltration membranes, J. Memb. Sci. 121 (1996) 71–82.
[25] W.R. Bowen, T.A. Doneva, H.-B. Yin, Separation of humic acid from a model surface water with PSU/SPEEK blend NF/UF membranes, J. Memb. Sci. 206 (2002) 417–429.
[26] T. Carroll, N.A. Booker, J. Meier-Haack, Polyelectrolyte-grafted microfiltration membranes to control fouling by natural organic matter in drinking water, J. Memb. Sci. 203 (2002) 3–13.
[27] A. Akthakul, R.F. Salinaro, A.M. Mayes, Antifouling polymer membranes with subnanometer size selectivity, Macromolecules 38 (2004) 7663–7668.
[28] K.M. Persson, V. Gekas, G. Trägardh, Study of membrane compaction and its influence on ultrafiltration water permeability, J. Memb. Sci. 100 (1995) 155–162.
[29] J. Marchese, P. Pradanos, N.A. Ochoa, M. Ponce, L. Palacio, A. Hernández, Fouling behaviour of polyethersulfone UF membranes made with different PVP, J. Memb. Sci. 211 (2003) 1–11.
[30] M. di Luccio, C. Borges, R. Nobrega, A. Habert, Microporous membranes by phase inversión I PC/NMP/water systems, Proc. II Iberoamerican Cong. Sci. Technol. Memb. (1994) 45–52.
[31] K.J. Kim, A.G. Fane, M. Nystrom, A. Pihlajamaki, W.R. Bowen, H. Mukhtar, Evaluation of electroosmosis and streaming potential for measurements of electric charges of polymeric membranes, J. Memb. Sci. 116 (1996) 149–159.
[32] A. Martin, F. Martinez, J. Malfeito, L. Palacio, P. Prádanos, A. Hernández, Zeta potential of membranes as function of pH: optimization of isoelectric point evaluation, J. Memb. Sci. 213 (2003) 225–230.
[33] K. Rodemann, E. Staude, Electrokinetic characterization of porous membranes made from epoxidized polysulfone, J. Memb. Sci. 104 (1995) 147–155.
[34] H.J. Jacobasch, M. Börner, Zur messung des Z-potentials platten –und folienförmiger polymere, Acta Polym. 34 (1983) 374–376.
[35] A. Szymczyk, B. Aoubiza, P. Fievet, J. Pagetti, Electrokinetic phenomena in homogeneous cylindrical pores, J. Colloid. Interface Sci. 216 (1999) 285–296.
[36] A. Mehta, A.L. Sydney, Permeability and selectivity analysis for ultrafiltration membranes, J. Memb. Sci. 249 (2005) 245–249.